12th International Conference on Integrated Diffuse Pollution Management (IWA DIPCON 2008).
Research Center for Environmental and Hazardous Substance Management (EHSM),
Khon Kaen University, Thailand ; 25-29 August 2008.

Measurements of Roof-deposit Load Under Rainy- and Non-rainy Conditions

Yasuo Nihei[1*] and Takushi Yoshida[2]

[1]Department of Civil Engineering, Tokyo University of Science, Chiba, 278-8510 Japan.

[2]Yachiyo Engineering Co., Ltd., Tokyo 161-8575, Japan.

[*]E-mail: nihei@rs.noda.tus.ac.jp

Abstract

To examine the temporal variation in the amount of roof deposit and its association with dry fallout, long-term continuous monitoring of roof-deposit environments is performed by a modeled-stormwater sampling (MOS) technique, by which one can easily obtain deposits from a model roof under simulated rainy conditions. The measured results indicate that the amount of sediment on the roof (SS_{roof}) decreases rapidly just after a rainfall and then increases gradually until the next rainfall occurs. The temporal variation in SS_{roof} is similar to that in the accumulated value of the deposition rate of suspended particulate matter (SPM), $\int D_{SPM}\,dt$.

Keywords: roof deposit, dry fallout, sediment, MOS technique, non-point source

1. Introduction

Aquatic environments in lakes and inner bays have been seriously polluted due to urbanization in its watershed and much of the waste of civilization. As measures for water pollutions, constructions of sewerage and regulation of industry waste water are valid and then point sources have been decreased significantly. In contrast, it is quite difficult to reduce non-point sources, which are distributed widely in the watershed like deposits on roads and roofs in urban areas[1],[2],[3],[4]. Therefore, it is important to appropriately evaluate the actual behavior of pollutants from non-point sources. In urban areas, where the increase of non-point sources has been significant, clarification of the yield and transport processes in the amount of road and roof deposits is crucial.

Field measurements for roof deposits, one of the main non-point sources in urban areas, have been conducted by collecting roof deposits by obtaining samples of stormwater flows from roof surfaces under natural rainy conditions. Although this method of collecting roof deposits may evaluate roof-deposit loads under rainy conditions, it is difficult to examine temporal variations of roof-deposit loads under rainy and non-rainy conditions. Therefore, appropriate models for roof-deposit load that incorporate its association with dry fallout, one of main production processes for non-point sources, do not exist.

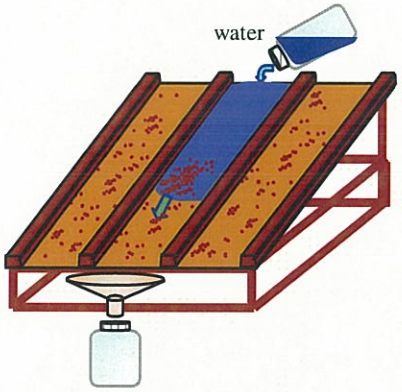

Figure 1. A schematic view of present sampling technique for roof deposits.

To examine the temporal variation in the amount of roof deposit and its relation to dry fallout, long-term continuous monitoring of roof-deposit environments is performed using a modeled-stormwater sampling (MOS) technique, by which deposits can easily be obtained from a model roof under simulated rainy conditions. By introducing this new monitoring technique, we may obtain the amount of roof deposits under rainy and non-rainy conditions, based upon which the relationship between roof-deposit environments and dry fallout can be discussed. The field measurement was conducted using model roofs mounted on top of our office building and the roof deposits were collected approximately once a day over half a year.

2. Monitoring Method of Roof-deposit Load

2.1 Outline of the Monitoring Technique

Using the previous technique of collecting roof deposits to evaluate the temporal variations in the amount of roof deposit is quite difficult under dry weather conditions. In the present study, we introduce a new monitoring technique for roof-deposit environments based on the following concepts:

1. Roof deposits are collected under simulated rainy conditions.
2. Daily variations of roof-deposit load are easily obtained.

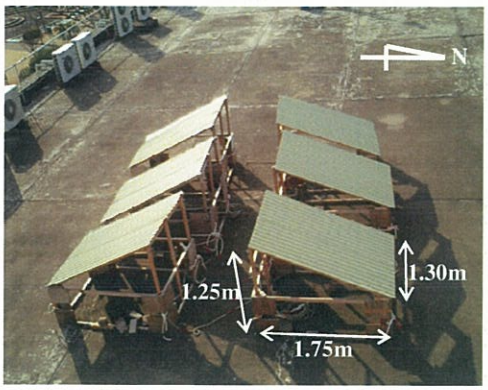

Figure 2. Photograph for model roofs used in the present monitoring technique.

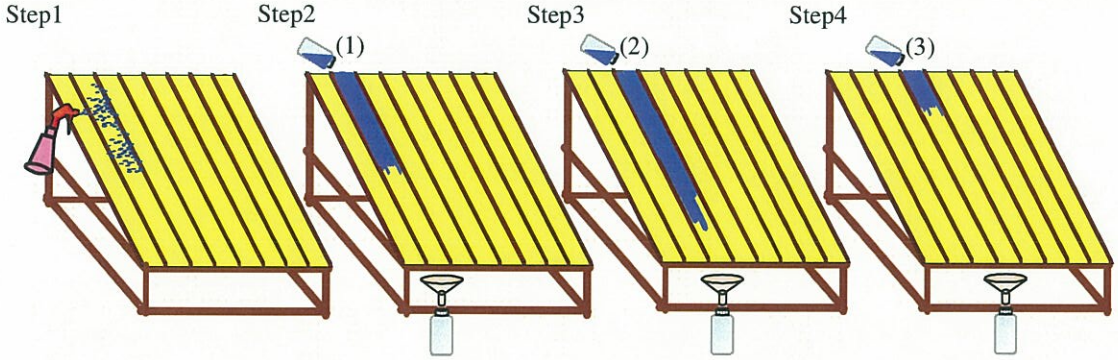

Figure 3. Procedure for collecting roof deposits in the present monitoring technique.

3. Field measurements are conducted with safety as a prerequisite.

Figure 1 shows a schematic view of the present monitoring method, which is designed based on the above concepts. In this technique, a model roof is used in order to ensure the safety of the field measurements. To collect roof deposits under simulated rainy conditions, water is poured onto the top of the model roof, and the water flowing off the bottom of the model roof is then sampled. The important concept with respect to the present technique is that only deposits suspended by the flowing water are collected. There are more than 15 ripples on the surface of each model roof, and in order to clarify the daily variations of roof deposits, different ripples were used for each measurement.
Figure 1 shows a schematic view of the present monitoring method. In this technique, a model roof is used in order to ensure the safety of the field measurements. To collect roof deposits under simulated rainy conditions, water is poured onto the top of the model roof, and the water flowing off the bottom of the model roof is then sampled. The important concept is that only deposits suspended by the flowing water are collected.

2.2 Procedure of the Present Monitoring Technique

The model roofs used in the present study, shown in Fig. 2, were constructed of galvanized sheet copper. Six roofs were set at an angle of 23 degrees on the roof of our office building. The dimensions of the model roofs were 1.25 m, 1.30 m, and 1.75 m, as shown in Fig. 2. We use three ripples in each measurement to reduce measurement errors. Figure 3 illustrates the procedures for collecting roof deposits in the present monitoring technique. The details of the procedure are as follows:

Step 1: Three ripples of the roof used in the measurement were moistened with an atomizer.
Step 2: A volume of 400 ml of water was poured onto the roof at the top edge in the first ripple and the running water was collected at the bottom of the roof.
Step 3: The collected water was then poured onto the roof at the top edge in the second ripple and the running water was collected at the bottom of the roof.
Step 4: The same procedure in Step 3 was performed in the third ripple.

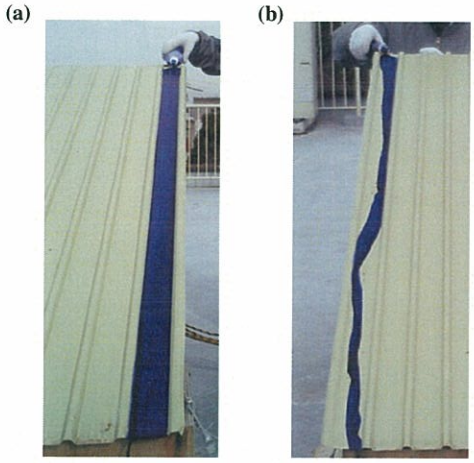

Figure 4. Flows on roofs with (left) and without (right) an atomizer.

For all of the water samples obtained, we measured turbidity using a nephelometer (WQC-24, DKK-TOA Co., Japan). We also analyzed the suspended solids (SS) and particle-size distribution for some of the water samples. The reason for using the atomizer in Step 1 is that the running water in the ripple flows uniformly after the roof surface is moistened by the atomizer as shown in Fig. 4.

2.3 Outline of Field Measurements

The model roofs were mounted on the roof of our office building, the position of which is indicated by the circle in Fig.5. The position is near a national highway. In order to examine the dependence of the roof deposits on the direction of the roof, we positioned the roofs to face north and south, as shown in Fig. 2. We selected three ripples of the roofs facing each direction, and a total of six ripples were used for each measurement of the roof-deposit environments. The measured results reveal that there was no appreciable difference in the deposits between the south-facing and north-facing roofs. Thus, we adopted the average of data obtained for the roofs for each direction.

The field measurements were performed approximately once a day, except on weekends and holidays. The observational period was from September 15 in 2005 to March 31 in 2006. We estimate the amount of the sediment on the roof per unit area, referred to herein as SS_{roof}, from the turbidity, which was measured for all water samples. The turbidity is converted to the SS using a calibration line between the turbidity and SS. SS_{roof} is defined as the SS divided by the area of the three ripples used in the measurement (= 0.297 m^2).

To compare the measured roof-deposit environments with atmospheric environments such as dry fallout, we measured the precipitation, air temperature, humidity, and wind speed, and the direction near the model roofs. In order to evaluate the dry fallout, we

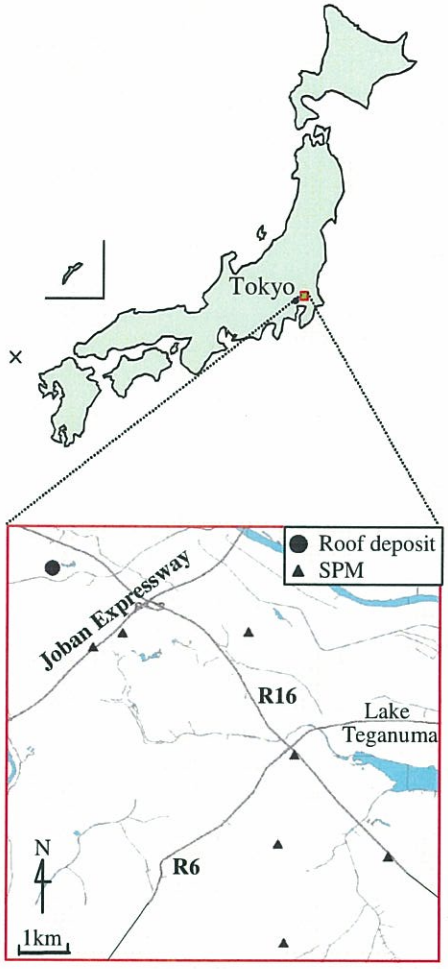

Figure 5. Locations of measurement stations for roof deposits and SPM.

also collected the observed data for suspended particulate matter (SPM), in which the particle diameter is less than 10 μm, from the database published by Ministry of the Environment in Japan. Here, we use the SPM measured at seven stations near our office, as depicted by the triangles in Fig. 5.

3. Measured Results and Discussion

3.1 Temporal Variation of SS_{roof}

In order to clarify the temporal variations of SS_{roof}, Figs. 6(a) and 6(b) show the time series of daily precipitation R and SS_{roof} over approximately half a year. There were no SS_{roof} data from December 19, 2005 to January 14, 2006, as the model roofs were damaged. The measured results indicate that the temporal changes of SS_{roof} are dominant and SS_{roof} varies from 0.0 to 0.25 g/m^2. The comparison of SS_{roof} and daily precipitation R indicates that the temporal variations of SS_{roof} are closely related to those of the daily precipitation, i.e., SS_{roof} decreases rapidly just after a rainfall and then increases gradually until the next rainfall occurs. In hydrologic events, an appreciable decrease in SS_{roof} was observed and the

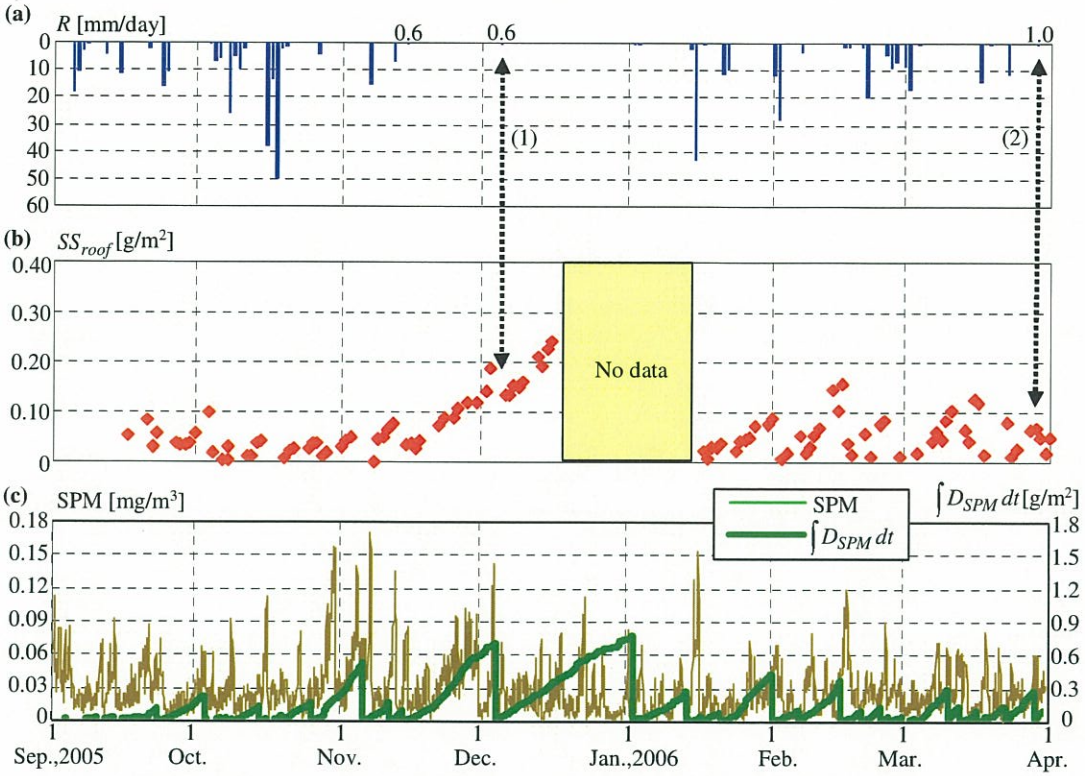

Figure 6. Temporal variations of daily precipitation R **(a)**, SS_{roof} **(b)** and SPM **(c)**.

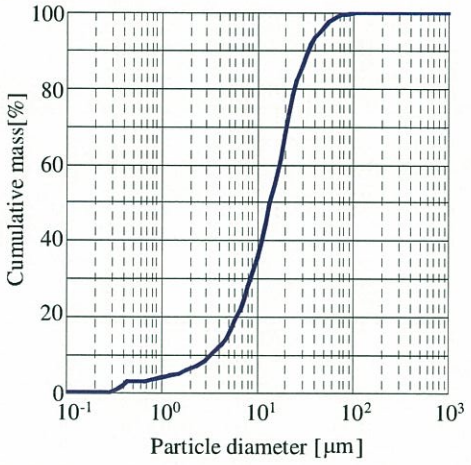

Figure 7. Grain-size distribution of roof deposits.

minimum values of SS_{roof} just after a rainfall were less than 0.05 g/m^2. However, the decreases in SS_{roof} were not large during periods of lower precipitation (*e.g.*, periods in which the daily precipitation was less than 1 mm) as indicated by the arrows in Fig. 6. Note also that the values of SS_{roof} in November and December, during which it did not rain continuously, were much larger than those in other periods.

3.2 Grain-size Distribution of Roof Deposit

In order to clarify the physical composition of the roof deposits, Fig. 7 shows the grain-size distribution of the roof deposits collected on November 30, 2005. The results indicate that the mean particle diameter is 13 μm and the fine particle of diameter of less than 30 μm occupies the majority of the roof deposits. It is confirmed that the mean particle diameter for other samples ranges from 12 μm to 15 μm, indicating a tendency similar to that observed in Fig. 7. These facts indicate that approximately half of the roof deposits are SPM and the other half are Particulate Matter (PM), the particle diameter of which is greater than 10 μm.

3.3 Relationship between SS_{roof} and Dry Fallout

In order to examine the relationship between SS_{roof} and SPM, the temporal variation of SPM is depicted in Fig. 6(c). In order to examine the effect of dry

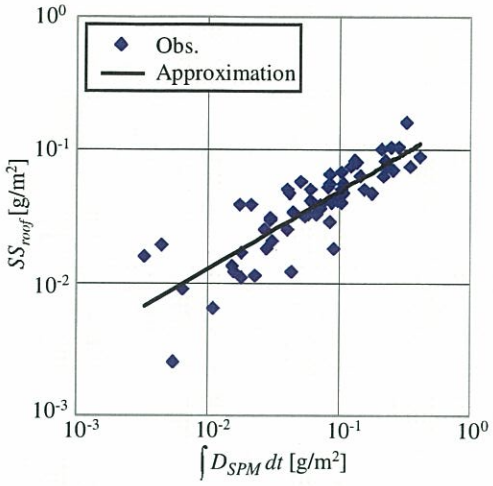

Figure 8. Relationship between SS_{roof} and $\int D_{SPM}\,dt$.

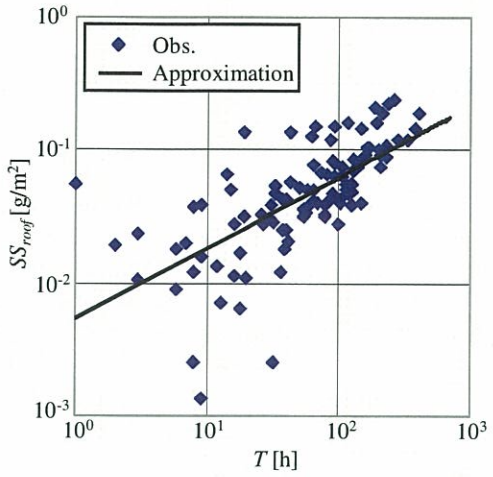

Figure 9. Relationship between T and $\int D_{SPM}\,dt$.

fallout from the atmosphere on the roof-deposit environments, we should examine not only SPM, but also PM, as discussed above. While the observed data set of SPM may be collected through the general database, we could not find a data set of PM observed in the vicinity of our office. Therefore, in the present study, we have examined only SPM. This figure reveals that the temporal variations of SPM are dominant, and its relationship to SS_{roof} remains unclear.

To directly compare SS_{roof} with the dry fallout, we evaluate the deposition flux of SPM on the roof, D_{SPM}, which is defined as

$$D_{SPM} = SPM * W_d , \qquad (1)$$

where W_d denotes a settling velocity of SPM, which is variously modeled in previous studies. Here, we obtain W_d using the terminal velocity of SPM in still air, W_0, and turbulent dispersion:

$$W_d = W_0 + 0.006u , \qquad (2)$$

where the turbulent dispersion is described in terms of wind velocity u. The unit of the velocities in the above equation is m/s. In line with the grain-size distribution of the roof deposits shown in Fig. 7, the terminal velocity W_0 is set at 3.1×10^{-3} m/s, using the Stokes equation for the particle diameter of 10 μm. Since the sediments on the roofs are regarded as a summation of dry fallout during a non-rainy period, the accumulated values of the deposition flux of SPM on the roof, $\int D_{SPM}\,dt$, are depicted in Fig. 6(c). In calculating $\int D_{SPM}\,dt$, we integrate D_{SPM} by setting $\int D_{SPM}\,dt$ to 0 just after a rainfall. The figure indicates that the temporal variations of $\int D_{SPM}\,dt$ are quite similar to those of SS_{roof}, showing a mutual relationship between $\int D_{SPM}\,dt$ and SS_{roof}.

Figure 8 illustrates the correlation between $\int D_{SPM}\,dt$ and SS_{roof} obtained in the present measurements. The observed data from the hydrologic event with daily precipitation of less than 1 mm until the next hydrologic event are not shown in the figure because $\int D_{SPM}\,dt = 0$ just after a rainfall is not valid. The figure represents the tendency for $\int D_{SPM}\,dt$ to increase with SS_{roof} on the whole. However, the correlation between SS_{roof} and $\int D_{SPM}\,dt$ varies widely for values of SS_{roof} of less than 0.03 g/m^2 due to the treatment of $\int D_{SPM}\,dt$ just after a rainfall. We obtain the approximation between $\int D_{SPM}\,dt$ and SS_{roof}, which is given as

$$SS_{roof} = 0.184\left(\int D_{SPM}\,dt\right)^{0.580} , \qquad (3)$$

where the unit of SS_{roof} and $\int D_{SPM}\,dt$ is g/m^2. The correlation coefficient between SS_{roof} and $\int D_{SPM}\,dt$ is 0.84, showing that the mutual relationship between SS_{roof} and $\int D_{SPM}\,dt$ is sufficiently estimated. This result demonstrates that we may accurately predict the roof-deposit environments from the dry fallout by using Eq. 3.

Although $\int D_{SPM}\,dt$ in Eq. 3 includes not only deposition flux of SPM but also the antecedent fine-weather hour T, which is the time after the rainfall, Fig. 8 does not clearly indicate the effects of SPM and T on the roof-deposit environments. The mutual relationship between SS_{roof} and T is shown in Fig. 9. Although the relationship between SS_{roof} and T varies widely, we obtain the approximation between them as follows:

$$SS_{roof} = 0.0041T^{0.574} , \qquad (4)$$

where the units of SS_{roof} and T are g/m^2 and hours, respectively. The coefficient of the correlation in Eq. 4 is 0.77, which indicates that the coefficient of correlation between SS_{roof} and T is smaller than that between SS_{roof} and $\int D_{SPM}\,dt$, demonstrating the importance of SPM on the evaluation of the roof-deposit environments.

Figure 10 illustrates the time series of SS_{roof} calculated with the observed $\int D_{SPM}\,dt$ and Eq. 3. The calculated SS_{roof} agrees well with the observed SS_{roof}. Therefore, the observed SPM and Eq. 3 can evaluate

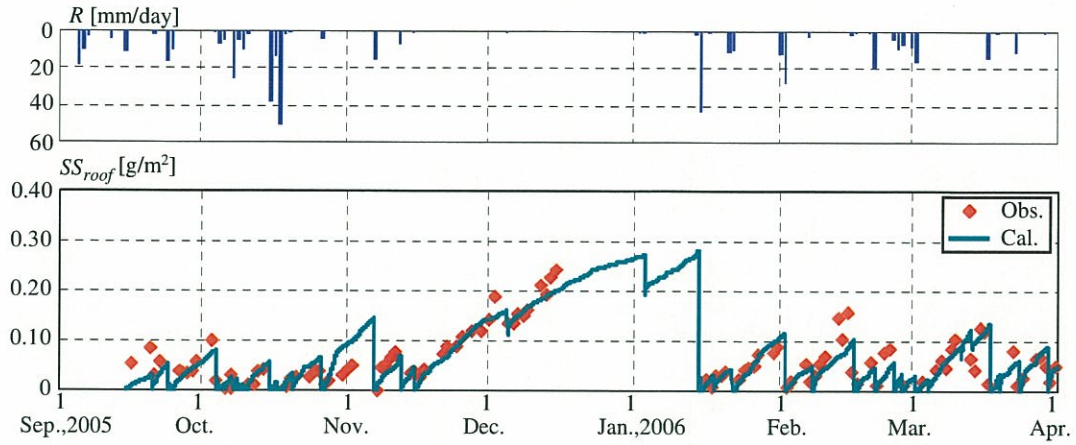

Figure 10. Comparison of temporal variations of the calculated and observed SS_{roof}.

the temporal variations of roof deposits under both rainy and non-rainy conditions. Since Eq. 3 decides the direct relationship between the atmospheric environments like SPM and the roof-deposit environments, we may indicate quantitatively the improvement of atmospheric environments for the reduction of non-point sources.

4. Conclusions

1) Long-term continuous monitoring of roof-deposit environments is performed by the modeled-stormwater sampling (MOS) technique, by which deposits can easily be obtained from the model roofs under simulated rainy conditions. By introducing this new monitoring method, we were able to obtain temporal variations of the amount of roof deposit under both rainy and non-rainy conditions.

2) The temporal variations of the sediments on the model roofs, SS_{roof}, are dominant and vary from 0 to 0.25 g/m^2. SS_{roof} decreases rapidly just after a rainfall and then increases gradually until the next rainfall occurs. In hydrologic events, the appreciable decreases in SS_{roof} are observed and the minimum values of SS_{roof} just after a rainfall were less than 0.05 g/m^2.

3) The correlation coefficient between SS_{roof} and $\int D_{SPM}\,dt$ is 0.84, showing that the mutual relationship between them is sufficiently estimated. Note that in order to obtain an accurate evaluation of the roof-deposit load, it is necessary to use $\int D_{SPM}\,dt$, in which the influences of antecedent fine weather conditions and dry fallout are explicitly incorporated.

Acknowledgments

This study was supported in part by the Japan Society for the Promotion of Science through a Grant-in-Aid for Scientific Research (C) (2) (No. 16560453). The authors would like to thank the students in the hydraulics laboratory of the Department of Civil Engineering, Tokyo University of Science, for their help in conducting the field observations of this study.

References

Book

[1] Weibel, S. R. 1969. Urban drainage as a factor in eutrophication, in *Eutrophication: Cause, Consequences and Correctives*, National Academy Science, Washington DC.

[2] Novotny, V. and Olem, H. 1994. Water quality: Prevention, Identification, and Management of Diffuse Pollution, Van Nostrand Rheinhold, New York.

[3]Butler, D. and Davies, J.W. 2000, Urban drainage, *Spon Press*.

[4]Welch, E.B. and Jacoby, J.M. 2004, Pollutant effects in freshwater, *Spon Press*.